ARL-TR-8644 ● FEB 2019

DEVCOM ARMY RESEARCH LABORATORY

Crystal Structure of Monohydrocalcite (Calcium Carbonate Monohydrate)-$CaCO_3 \cdot H_2O$ or $CaHCO_3(OH)$: A New Hydrogen-Stabilized Piezoelectric

by I Kohatsu and JW McCauley

Approved for public release; distribution is unlimited.

NOTICES

Disclaimers

The findings in this report are not to be construed as an official Department of the Army position unless so designated by other authorized documents.

Citation of manufacturer's or trade names does not constitute an official endorsement or approval of the use thereof.

Destroy this report when it is no longer needed. Do not return it to the originator.

ARL-TR-8644 ● FEB 2019

Crystal Structure of Monohydrocalcite (Calcium Carbonate Monohydrate)-$CaCO_3 \cdot H_2O$ or $CaHCO_3(OH)$: A New Hydrogen-Stabilized Piezoelectric

by I Kohatsu
US Army Materials and Mechanics Research Center,
National Research Council Postdoctorate Fellow, 1973

JW McCauley (Emeritus)
Weapons and Materials Research Directorate, ARL

Approved for public release; distribution is unlimited.

REPORT DOCUMENTATION PAGE

Form Approved
OMB No. 0704-0188

Public reporting burden for this collection of information is estimated to average 1 hour per response, including the time for reviewing instructions, searching existing data sources, gathering and maintaining the data needed, and completing and reviewing the collection information. Send comments regarding this burden estimate or any other aspect of this collection of information, including suggestions for reducing the burden, to Department of Defense, Washington Headquarters Services, Directorate for Information Operations and Reports (0704-0188), 1215 Jefferson Davis Highway, Suite 1204, Arlington, VA 22202-4302. Respondents should be aware that notwithstanding any other provision of law, no person shall be subject to any penalty for failing to comply with a collection of information if it does not display a currently valid OMB control number.
PLEASE DO NOT RETURN YOUR FORM TO THE ABOVE ADDRESS.

1. REPORT DATE *(DD-MM-YYYY)*	2. REPORT TYPE	3. DATES COVERED (From - To)
February 2019	Technical Report	1 November 1973–14 November 2018

4. TITLE AND SUBTITLE

Crystal Structure of Monohydrocalcite (Calcium Carbonate Monohydrate)- $CaCO_3 \cdot H_2O$ or $CaHCO_3(OH)$: A New Hydrogen-Stabilized Piezoelectric

5a. CONTRACT NUMBER

5b. GRANT NUMBER

5c. PROGRAM ELEMENT NUMBER

6. AUTHOR(S)

I Kohatsu and JW McCauley

5d. PROJECT NUMBER

5e. TASK NUMBER

5f. WORK UNIT NUMBER

7. PERFORMING ORGANIZATION NAME(S) AND ADDRESS(ES)

Army Research Laboratory
ATTN: RDRL-WMM
Aberdeen Proving Ground, MD 21005-5069

8. PERFORMING ORGANIZATION REPORT NUMBER

ARL-TR-8644

9. SPONSORING/MONITORING AGENCY NAME(S) AND ADDRESS(ES)

US Army Materials and Mechanics Research Center
Watertown, MA 02472

10. SPONSOR/MONITOR'S ACRONYM(S)

11. SPONSOR/MONITOR'S REPORT NUMBER(S)

12. DISTRIBUTION/AVAILABILITY STATEMENT

Approved for public release; distribution is unlimited.

13. SUPPLEMENTARY NOTES

14. ABSTRACT

Single crystals of $CaCO_3 \cdot H_2O$ were synthesized by a silica-gel technique using the following reaction with sugar ($C_{12}H_{22}O_{11}$) added: $Na_2CO_3 + CaCl_2 = CaCO_3 + 2NaCl$. Precession and Weissenberg X-ray diffraction photographs indicated one of two enantiomorphic polar space groups, $P3_121$ or $P3_221$, which should exhibit piezoelectricity. The subcell lattice parameters are a = 6.092(2) Å and c = 7.529(2) Å with three formula units in the unit cell. The presence of very weak superstructure-type reflections indicated that the real structure has a tripled unit cell with $[a_s,b_s,c_s] = [(1/3\ 1/3\ 0)\ (-1/3\ 2/3\ 0)\ (0\ 0\ 1)][a_o,b_o,c_o]$. The substructure, assuming half occupancy of carbon and oxygen in general positions, refined to an R factor of 3.4% using anisotropic temperature factors. Ca is surrounded by eight oxygens at distances of 2.42–2.49 Å. One extraordinarily long C-O distance in the carbonate group, 1.367 Å, compared with the other two of 1.251 and 1.273 Å, suggested that hydrogen was bonded to it forming an HCO_3 anion, also suggested by the infrared absorption spectra. The structure is further characterized by disordered CO_3 groups, pointing up and down the c axis. The superstructure is proposed to result from the ordering of the carbonate groups.

15. SUBJECT TERMS

calcium carbonate monohydrate, crystal growth, crystal structure analysis, vaterite, piezoelectricity

16. SECURITY CLASSIFICATION OF:			17. LIMITATION OF ABSTRACT	18. NUMBER OF PAGES	19a. NAME OF RESPONSIBLE PERSON
a. REPORT	b. ABSTRACT	c. THIS PAGE			JW McCauley
Unclassified	Unclassified	Unclassified	UU	30	19b. TELEPHONE NUMBER (Include area code) (410) 306-0711

Standard Form 298 (Rev. 8/98)
Prescribed by ANSI Std. Z39.18

Contents

List of Figures iv

List of Tables iv

Preface v

1. Introduction 1

2. Experimental 3

3. Structure Determination 4

4. Discussion of Substructure 5

5. Discussion of Superstructure Determination 12

6. Preliminary Discussion of Vaterite-Calcium Carbonate Monohydrate Relationships 13

7. References 17

Appendix A. Figure of Structure Factor Tables 19

Appendix B. $CaCO_3 \cdot H_2O$ Optical Photomicrographs 21

Distribution List 23

List of Figures

Fig. 1 Calcium carbonate monohydrate crystals 2

Fig. 2 Original notebook drawing of crystal-growth experimental arrangement..... 2

Fig. 3 Silica-gel vaterite spherulites grown at a pH of 7.5 with 0.65 M $CaCl_2$ + 0.36 M Na_2CO_3 3

Fig. 4 Precession X-ray diffraction along [110]..... 3

Fig. 5 Ca coordination with eight oxygen atoms 8

Fig. 6 Detailed Ca coordination with bond lengths..... 9

Fig. 7 Orientation of carbonate (CO_3) groups with C-O bond lengths along the 3_2 axis..... 10

Fig. 8 Orientation of the $(OH)^-$ dipole following that of HCO_3 11

Fig. 9 X-ray powder diffraction patterns of vaterite and $CaCO_3 \cdot H_2O$..... 13

Fig. 10 Infrared spectra of $CaCO_3 \cdot H_2O$..... 14

Fig. 11 Infrared spectra of the vaterite, calcite, and aragonite 14

Fig. A-1 Image shows tables of observed and calculated structure factors based on final atomic parameters..... 20

Fig. B-1 $CaCO_3 \cdot H_2O$ in transmitted plane light..... 22

Fig. B-2 Halved crystal in crossed polarized light 22

Fig. B-3 Magnified image of halved crystal with apparent inclusions 22

List of Tables

Table 1 Crystallographic data of $CaCO_3 \cdot H_2O$ or $CaHCO_3(OH)$ 4

Table 2 Atomic parameters of $CaCO_3 \cdot H_2O$ in substructure[a] 5

Table 3 Metal–oxygen distances Å..... 6

Table 4 Oxygen–oxygen contact distances Å 6

Table 5 Polyhedral-bond angles (degrees)..... 7

Table 6 Infrared absorption spectra of $CaCO_3$ H_2O..... 15

Preface

This paper was completed in draft form in 1973 but never completely finalized. Dr Kohatsu left the US Army Materials and Mechanics Research Center that year and I had two major surgeries over the next two years, so the draft was left unfinished. Only an extended abstract ("Evidence of Carbonate Order-Disorder in $CaCO_3 \cdot H_20$" by I Kohatsu and JW McCauley, American Crystallographic Association, January 1973) was published. I thought that it would be important to archive the current imperfect version of the paper for future reference.

Approved for public release; distribution is unlimited.

1. Introduction

Calcium carbonate monohydrate ($CaCO_3.H_2O$, $CaHCO_3(OH)$, monohydrocalcite) has been found in a wide variety of occurrences: Portland-cement reaction products[1]; calcareous encrustations in Lake Issyk-Kul, Kirgizstan[2]; otoliths (concretions in inner ear) of a tiger shark[3]; air-conditioning unit deposits[4]; in natural deposits (speleothems)[5] by an evaporation-aerosol mechanism; a biochemical process[6]; lake deposits[7]; and in a guinea-pig bladder stone.[8] It has also been synthesized by other investigators.[9–13] Various impurities like polyphosphates, magnesium compounds, and some organic chemical additives, like sugar, and low temperature are known to favor the formation of this substance. Evidence was also found by McCauley and Roy[13] that there seemed to be an intimate relationship between the vaterite polymorph of $CaCO_3$ and $CaCO_3.H_2O$. Further, it also seemed that in precipitation media with exceedingly high Ca concentration, $CaCO_3$ H_2O nucleates first, but quickly becomes poisoned with the subsequent overgrowth of spherulitic vaterite. McCauley[12] also recognized a strong similarity between the X-ray powder diffraction patterns and lattice parameters of vaterite and $CaCO_3.H_2O$. Moreover, vaterite spherulites can contain large amounts of water in intimate association.[14] Finally, McConnel[15] pointed out that vaterite appears to be the end member (crystal structure and optical properties) of the bastnaesite (Ce FCO_3)–synchisite ($CeFO_3.CaCO_3$) solid solution series. All of these results seem to imply that vaterite and calcium carbonate monohydrate have some sort of intrinsic relationship.

In previous work[12,13] on the controlled crystal growth of various $CaCO_3$ phases in a silica-gel environment, the following reaction was used: $Na_2CO_3 + CaCl_2 = CaCO_3 + 2NaCl$. Equal volumes of 0.5N acetic acid and 1 N of Na_2CO_3 were added to gel a water-glass liquid (a generic name for chemical compounds with the formula $Na_{2x}SiO_{2+x}$); a 1-M solution of $CaCl_2$ was added to the top of the gel. As the $CaCl_2$ solution diffused into the silica gel various forms of $CaCO_3$ precipitated from the gel. It was found that a monohydrate phase was formed when a small amount of sugar ($C_{12}H_{22}O_{11}$) was added.[12] Figure 1 illustrates the single crystals that were rounded trigonal bipyramids, typically about 0.5 mm in diameter. Figure 2 is an original notebook drawing of the experimental arrangement and the distribution of various crystals.

Approved for public release; distribution is unlimited.

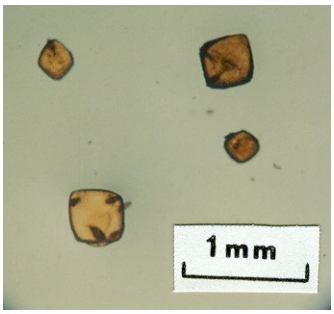

Fig. 1 Calcium carbonate monohydrate crystals

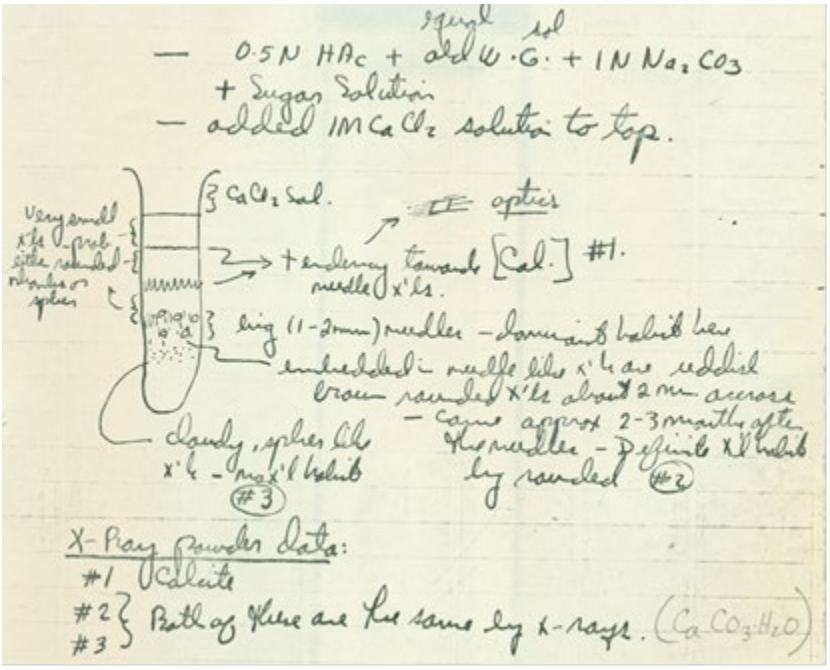

Fig. 2 Original notebook drawing of crystal-growth experimental arrangement

Lippman[16] proposed from his single-crystal X-ray diffraction patterns that it was trigonal, a_o = 10.62Å and c_o = 7.54 Å with Z = 9 and either P3 $_{(1, 2)}$21 or P3 $_{(1, 2)}$ 12 as possible space groups. He also reported it had a pronounced pseudo cell with a^*_o = 6.13 Å = a_o/3½ and c_o = 7.54 Å with Z = 3. Thus, further structural analysis may be important for the elucidation of precise atomic arrangement and, thereby, for the comparison with anhydrous carbonates such as calcite, aragonite, and vaterite, and with other known hydrated calcium carbonates like $CaCO_3 \cdot 6H_2O$ (Ikaite). Figure 3 illustrates examples of vaterite spherulites grown in the previous study.

Approved for public release; distribution is unlimited.

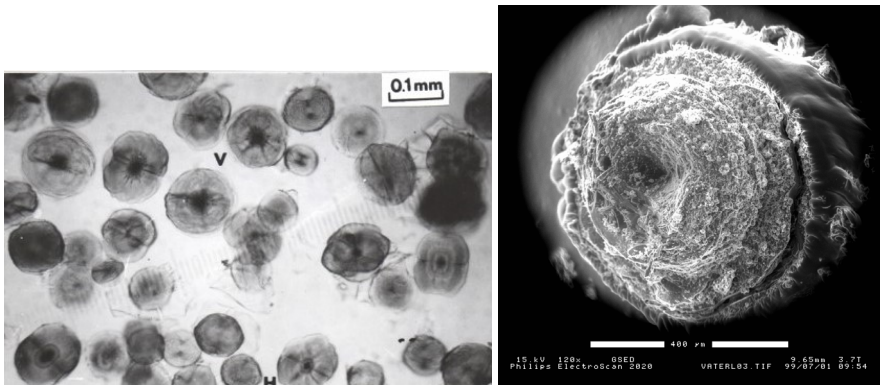

a. Transmitted light photomicrograph of Vaterit b. SEM of fractured vaterite spherulite-scale = 400 µm

Fig. 3 Silica-gel vaterite spherulites grown at a pH of 7.5 with 0.65 M $CaCl_2$ + 0.36 M Na_2CO_3

2. Experimental

From the single-crystal X-ray diffraction precession and Weissenberg photographs, it was confirmed that the structure based on all strong reflections (substructure) was trigonal with a two-fold axis being normal to (110). Figure 4 is an X-ray single-crystal precession diffraction pattern in the [110] direction illustrating the two-fold (diad) axis of symmetry. This photograph is a direct representation of the reciprocal lattice.

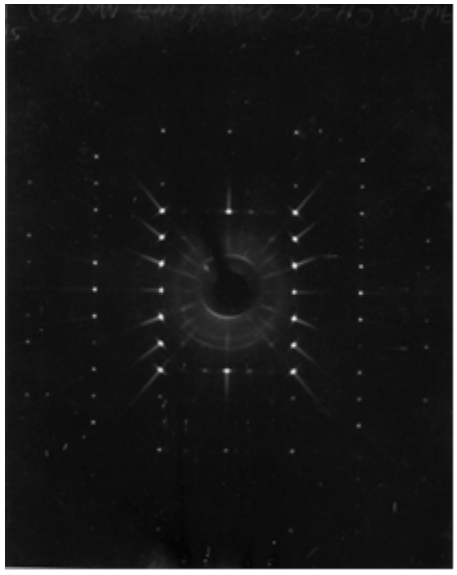

Fig. 4 Precession X-ray diffraction along [110]

Systematic extinctions were found for (00ℓ) reflections with $\ell \neq 3n$; therefore, the space group was reduced to either $P3_121$ or $P3_221$ from the four space groups,

$P3_{(1,2)}21$ and $P3_{(1,2)}12$, proposed by Lipman.[16] When weak reflections, which were observable only for overexposed photographs, are included, the structure (superstructure) was proved to have tripled unit cell, $[a_s,b_s,c_s] = [(1/3\ 1/3\ 0)\ (-1/3\ 2/3\ 0)\ (0\ 0\ 1)]\ [a_o,b_o,c_o]$ of the substructure. Since the unit cell of the superstructure is derived by 30° rotation along c, the two-fold axis is now normal to (100) of super cell; this leads to $P3_121$ and $P3_212$ as possible space group for the superstructure. However, our conclusion is that the correct one is $P3_2$ or $P3_1$ without a two-fold axis. The precision lattice constants were obtained by a Nelson–Riley extrapolation technique using (hk0) and (00ℓ) reflections recorded on a back-reflection Weissenberg camera with polychromatic X radiation. The result is shown in Table 1. The calculated density based on these lattice parameters is 2.42 g/cc, which agrees with a measured density of 2.38 g/cc using a Berman density balance.

Table 1 Crystallographic data of $CaCO_3 \cdot H_2O$ or $CaHCO_3(OH)$

	Subcell	Supercell
System	Trigonal	Trigonal
Crystal morphology	Trigonal bipyramid	…
Space group	$P3_221$ or $P3_121$	$P3_2$ or $P3_1$ [a]
Lattice constants Å [b]	a = 6.092(2)	a = 10.552(2)
	c = 7.529(2)	c =7.529(2)
Unit cell formula units	Z = 3	Z = 9
Density (g/cm^3)	ρ_c = 2.43	…
	ρ_{ob} = 2.38	…

[a] Lippman.[16]

[b] Precision lattice constants obtained by Nelson–Riley extrapolation technique.

The diffraction intensity data were collected for the substructure using a manual Picker four-circle goniometer with unfiltered MoK_α. The diffraction peaks were scanned for 12° (2θ) around the maximum by a 2θ-ω scan at the rate of 1°/min. The background was counted before and after the scan for 20 s. The standard deviations were calculated using normal counting statistics. The intensities were corrected for Lorentz-polarization factors, but absorption and extinction corrections were not needed. Among the 290 measured reflections, only four were deemed unobservable.

3. Structure Determination

The substructure was determined using 286 observable reflections. A Patterson map was calculated by FORDAP and the heavy Ca atoms were located at special position 3a of space group $P3_221$. The R factor (percent relation of observed structure factors F_o to calculated structure factors F_c: F_o/F_c) was 30% after refining

the Ca positions by the least-squares program RFINE. A Fourier map, calculated from the observed structure factors with phases assigned from Ca positions, showed that O (1) and O (2) were located at special position 3b and general position 6c respectively. The phases of F_c were redetermined including these atoms and the difference map was calculated. There were two pairs of split peaks around the special positions and they were assigned as O (3) and C with a half occupancy. After the refinement of all these positional parameters, the R value decreased to 9.5% with isotropic temperature factors B = 1.O $Å^2$ for all atoms. The further refinement with anisotropic temperature factors for O (3) and C finally reduced R to 3.6%, and the weighted R reduced the counting statistics error to 3.9%. Including four unobservable reflections, R and the weighted R became 4.4% and 4.7% respectively. The final atomic parameters are shown in Table 2. The observed and calculated structure factors based on these parameters are shown in Appendix A.

Table 2 Atomic parameters of $CaCO_3 \cdot H_2O$ in substructure[a]

	x	y	z	B_{11}	B_{22}	B_{33}	B_{12}	B_{13}	B_{23}
Ca	0.2776(2)	0	2/3	0.0060(3)	0.0080(6)	0.0060(2)	0.0040(6)	0.0001(2)	0.0002(2)
Ox (1)	0.6028(9)	0	1/6	0.0090(15)	0.0118(23)	0.0098(10)	0.0059(23)	–0.0019(7)	–0.0038(7)
Ox (2)	0.1856(7)	0.7290(7)	0.4059(4)	0.0090(16)	0.0147(15)	0.0095(6)	0.0069(12)	–0.0024(8)	–0.0031(8)
Ox (3)	0.9376(14)	0.8825(14)	0.4539(8)	1.68(16)	…	…	…	…	…
C[b]	0.2773(21)	0.2599(20)	0.0441(12)	1.35(21)	…	…	…	…	…

Notes: Ox (1) is in special position 3b, Ox (2) in general position 6c, both part of CO_3; Ca in special position 3a. βij = anisotropic temperature factors.
[a] Based on 284 observed reflections: R= 3.4%.
[b] Half occupancy was assumed.

4. Discussion of Substructure

The interatomic distances and angles for Ca and C polyhedra are presented in Tables 3–5. Ca is coordinated by eight oxygens with interatomic distances from 2.418 Å to 2.490 Å. Figures 5 and 6 illustrate the Ca coordination with oxygen and the relevant bond distances.

Table 3 Metal–oxygen distances Å

Cation	Oxygen	Cation-oxygen Interatomic distance
Ca-	0 (3)'	2.418 (8)
	0 (3)	2.426 (8)
	0 $(2)^{II}$	2.443 (3)
	0 $(2)^{II}$	2.456 (4)
	0 $(1)^{II}$	2.490 (3)
H(1)-	$0(2)^{IV}$	…
	$0(1)^{II}$	…
H(2)-	$0(1)^{II}$	…
	$0(2)^{V}$	…
C -	0(2)	1.237 (14)
	0(3)	1.273 (10)
	$0(2)^{IV}$	1.377 (14)

Table 4 Oxygen–oxygen contact distances Å

	Oxygen—oxygen	Interatomic distances	
1)	Ca-O polyhedron (dodecahedron)		
	0(3) – 0(2)	2.16 (8)	C
	$0(2)^{11} – 0(2)^{111}$	2.243 (7)	C
	$0(3)^{1} – 0(3)$	2.730 (5)	…
	$0(2)^{1} – 0(3)^{1}$	2.913 (9)	…
	$0(1) – 0(2)^{111}$x2	2.976 (3)	…
	$0(3)^{1} –$ 0(1) x2	3.002 (8)	…
	$0(2)^{11} – 0(2)^{1}$x2	3.191 (4)	…
	$0(1)^{1} – 0(3)^{1}$	3.288 (10)	…
	0(1) – 0(2) x2	3.370 (4)	…
	$0(2) – 0(2)^{111}$x2	3.390 (3)	…
	0(1) – 0(3)	3.444 (8)	…
	$0(2)^{1} –$ 0(1) x2	3.672 (5)	…
	$0(3) – 0(2)^{111}$	4.344 (9)	…
	$0(3)^{1} – 0(2)^{11}$	4.471 (9)	…
2)	C-O polyhedron (triangle)		
	0(3) – 0(2)	2.16 (9)	Ca
	$0(2) – 0(2)^{IV}$	2.243 (7)	Ca
	$0(2)^{IV} –$ 0(3)	2.426 (8)	…

Approved for public release; distribution is unlimited.

Table 5 Polyhedral-bond angles (degrees)

1)	Ca-O-O Polyhedron	
	0(2) – 0(3)	52.9 (2)
	$0(2)^{11}$ – $0(2)^{111}$	54.4 (2)
	0(3) – $0(3)^{1}$	68.6 (1)
	$0(2)^{1}$ – $0(3)^{1}$	73.6 (2)
	0(1) – $0(2)^{111}$ x2	74.0 (1)
	$0(1)^{1}$ – 0(3)	75.3 (2)
	0(1) – $0(3)^{1}$	75.4 (2)
	0(2) – $0(2)^{111}$x2	81.3 (1)
	$0(1)^{1}$ – $0(3)^{1}$	84.1 (2)
	0(1) – 0(2) x2	86.2 (1)
	0(2) – $0(2)^{11}$x2	87.6 (1)
	0(1) – 0(3)	88.9 (2)
	0(1) – $0(2)^{1}$x2	96.2 (1)
	0(2) – $0(3)^{1}$	118.7 (2)
	$0(2)^{11}$ – 0(3)	125.7 (2)
	0(1) – $0(2)^{11}$x2	128.3 (1)
	$0(2)^{111}$ – 0(3)	132.3 (2)
	$0(2)^{1}$ – 0(3)	139.2 (2)
	$0(2)^{111}$ – $0(3)^{1}$	141.9 (2)
	$0(2)^{11}$ – $0(3)^{1}$	147.7 (2)
	0(1) – $0(1)^{1}$	157.7 (2)
	0(2) – $0(2)^{1}$	167.5 (2)
2)	C-O Polyhedron	
	$0(2)^{11}$ – 0(2)	118.1 (6)
	0(2) – 0(3)	119.5 (12)
	$0(2)^{11}$ – 0(3)	122.4 (12)
3)		
	H(1) – 0(1) H(2)	106.6 (2)

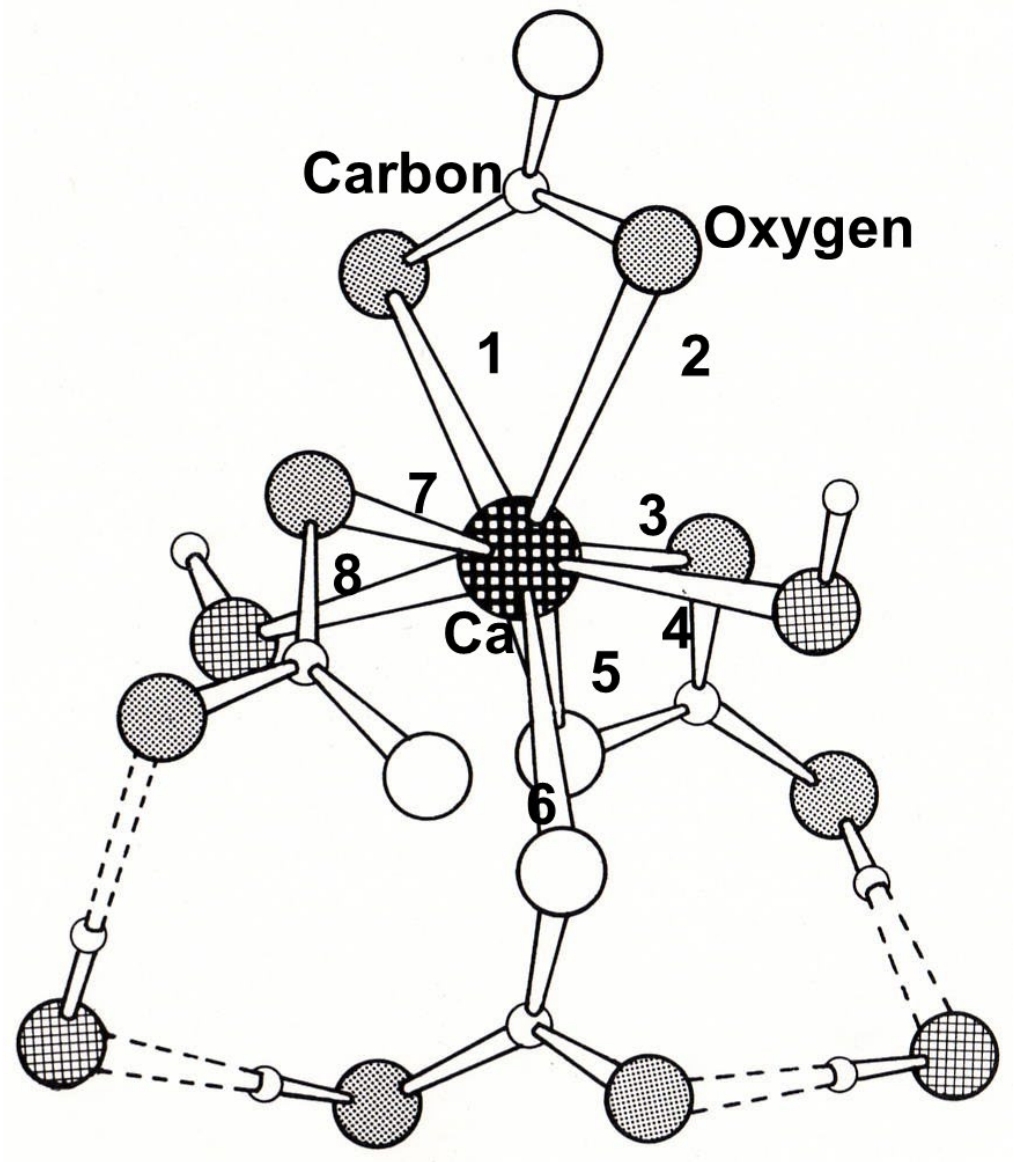

Fig. 5 Ca coordination with eight oxygen atoms

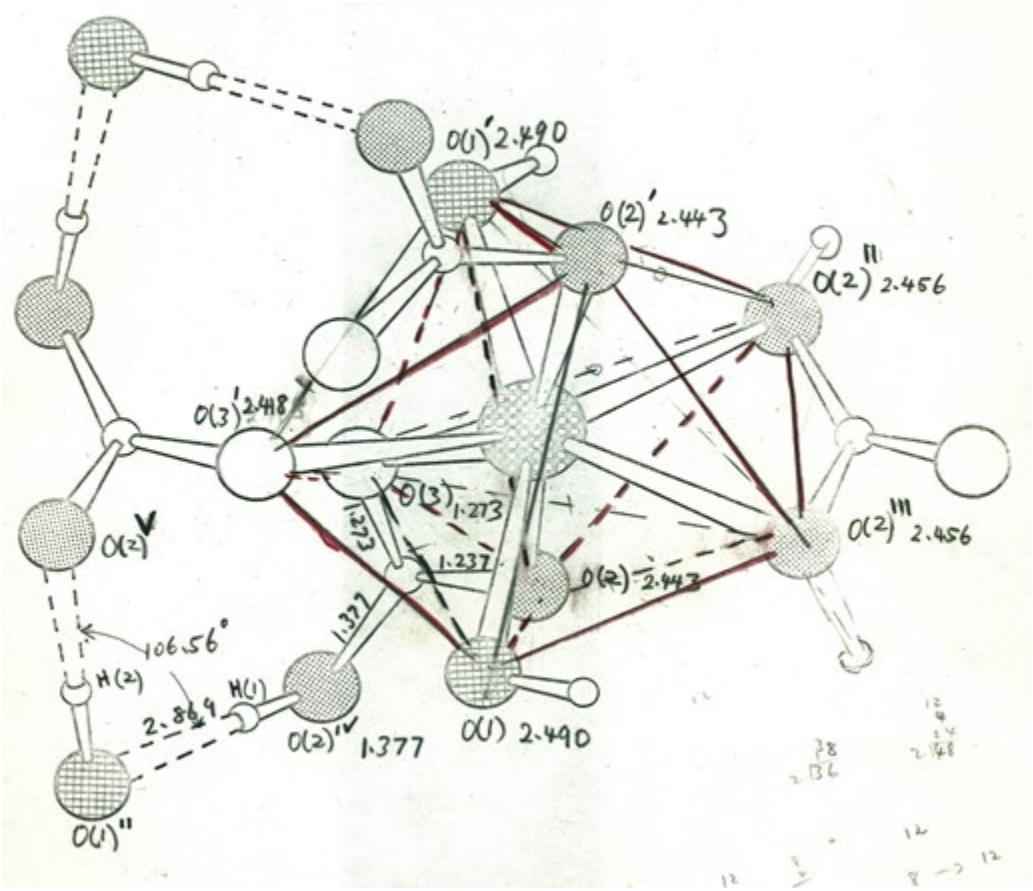

Fig. 6 Detailed Ca coordination with bond lengths

The carbonate group is very irregular—much like $NaHCO_3$, C-O of O (2), and O (3) and O (2) ^{IV} distances of 1.24 Å, 1.27 Å, and 1.377 Å—but the three O-C-O angles are quite regular at 118°, 120°, and 122°. This irregularity in C-O distances is quite different from other Ca carbonate compounds such as calcite, aragonite, and $CaCO_3 \cdot 6H_2O$, where all three C-O distances are equal or nearly equal. However, the same case is found in the structure of $NaHO_3$,[17] where three C-O distances are 1.249Å, 1.275 Å, and 1.345Å, and in vaterite.[18] In $NaHCO_3$, the longest C-O corresponds with oxygen, which is bonded to hydrogen. Therefore, by analogy, it is proposed that a hydrogen H (1) is associated with O $(2)^{IV}$ forming an HCO_3-like anion in this structure and it must be located along the O $(1)^{II}$ – $0(2)^{IV}$ join, because this is the only O – O join that is the edge of neither the Ca-O nor the C-O polyhedron. Disordering of O (3) and C again makes no change in the CO_3 geometric shape because a diad axis bisects the O $(2)^{II}$ – O $(2)^{IV}$ edge, and the disordered sites are related with the diad axis. However, the orientation of the CO_3 plane changes along the 3_2 axis depending on whether O (3) and C together take upper (+) or lower (–) sites with respect to the diad axis as shown in Fig. 7.

Approved for public release; distribution is unlimited.

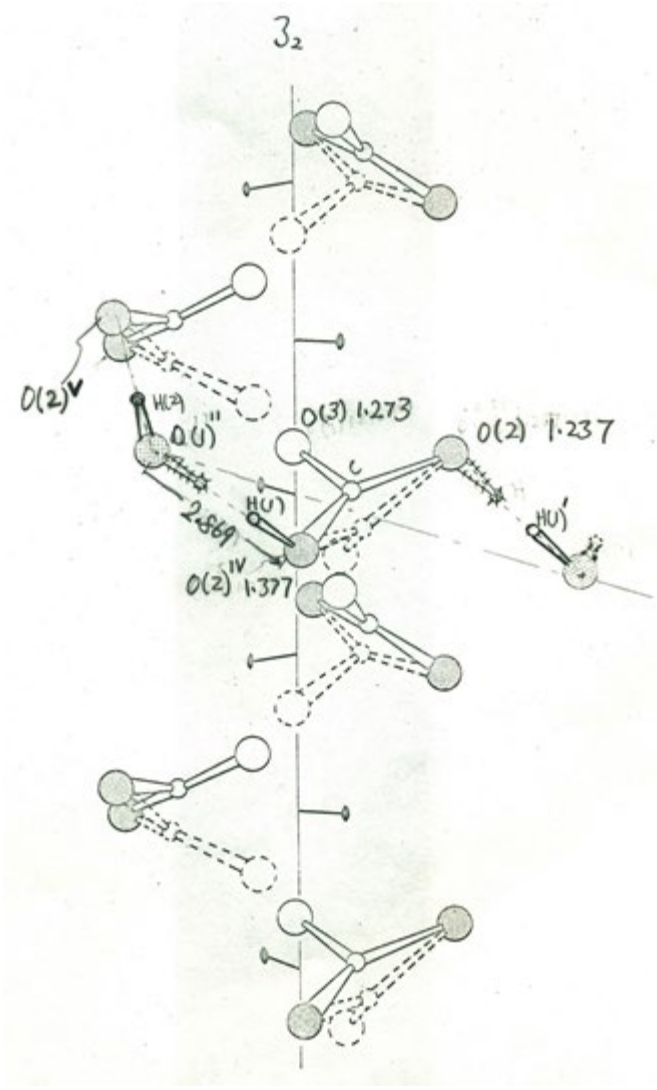

Fig. 7 Orientation of carbonate (CO_3) groups with C-O bond lengths along the 3_2 axis

Accordingly, H (1) is in a general position and O $(1)^{II}$ – O $(2)^{IV}$ have a half occupancy on each site. It is, then, necessary to place three more hydrogens either in special positions or in a general position with a half occupancy. The only possible site is a general position along O $(1)^{II}$ – O $(2)^{IV}$ join. That is when H (1) is on O $(1)^{11}$ – O $(2)^{IV}$, the second hydrogen H (2) is located at O $(1)^{II}$ – O $(2)^{V}$ and possibly bonded to O $(1)^{11}$ (water oxygen) to form an OH^- anion. Therefore, H (2) also is statistically distributed, and the OH^- shape remains the same, but the orientation of OH^- dipole follows that of HCO_3 (see Fig. 8).

Approved for public release; distribution is unlimited.

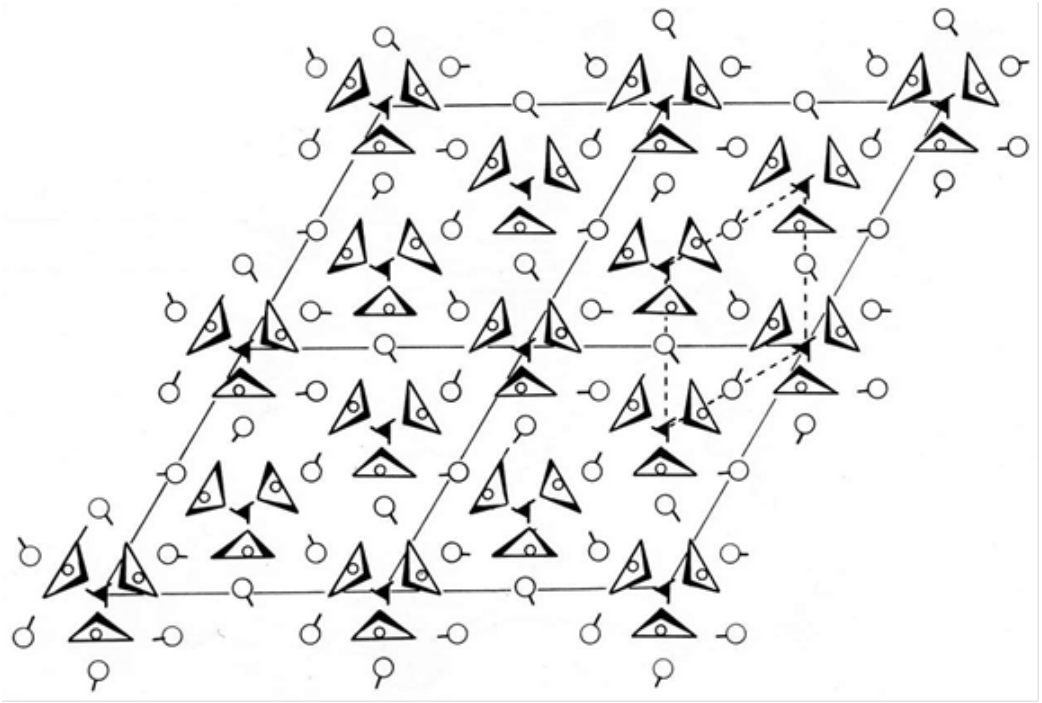

Fig. 8 Orientation of the $(OH)^-$ dipole following that of HCO_3

The hydrogen-bonding scheme may be further examined with respect to the environment of O (1)[11] (Fig. 6). The O (1) is surrounded tetrahedrally by two Ca's and two CO_3 oxygens. All of the angles are within 4° from the ideal tetrahedral angle, 109.47°, except 2Ca-O-Ca, 101.6° (Table 5). The two CO_3 oxygens are associated to O (1) through hydrogen bonding. If Pauling's rule is applied, O (1) receives 2 × (+1/4) = +1/2 from 8 coordinated positive divalent Ca ions. This requires O (1) to receive +1.5 more charges from two positive hydrogen ions. Since H (2) is strongly bonded to O (1) the contribution to O (1) is assumed to be close to +1. However, H (1) is closely associated with CO_3, but also with O (1), the contribution to O (1) may be +0.5 to make up the rest. Thus, the inequality of C-O distances is exactly compared with the asymmetric aspect of the water molecule. In the substructure, which is now better described as an *average structure*, the hydrogen appears to be oscillating between $O(1)^{II}$ and $O(2)^{IV}$; OH-O and O-HO as the CO_3 plane takes upward or downward orientations. This is not a thermal effect because the spacings of the disordered oxygen and carbon sites are 0.90 Å and 0.69Å respectively, which are too large for the thermal vibration amplitude. Therefore, in a whole structure, the orientations of CO_3 planes are random. But, it is not completely random because CO_3 planes along the same 3_2 axis must have the same orientation, otherwise the O (3) – O (3) distance between neighboring CO_3 planes of opposite orientation becomes an unreasonable 1.93 Å compared with a more reasonable 2.73 Å for the same orientation. Thus, there are two kinds of unit

cells, one with CO_3 oriented upward (+ cell) and the other downward (– cell). Although each unit cell lacks a diad axis, the overall structure will have a diad axis because of the statistical distribution of + and – cells.

The overall structural scheme in the + or – cell is characterized by an infinite CO_3 spiral chain along the 3_2 axis interconnected through an H-0-H bond. Each CO_3 plane is shared with two Ca-dodecahedrons by two shorter edges (2.168 Å × 2.243 Å). A Ca-dodecahedron is surrounded by two CO_3 planes sharing edges, two CO_3 by corners sharing and two H-O-H's at the corners.

5. Discussion of Superstructure Determination

Since the superstructure reflections are very weak, the deviation from the substructure must be extremely subtle and difficult to detect by X-ray diffraction. This leads us to believe the superstructure is formed because of the ordering of two different CO_3 orientations, which are very close with each other. There are two schemes in the superstructure formation because of two crystallographically independent ways to place a superstructure origin in a substructure (i.e., (000) and at (1/3 2/3 0) or (2/3 1/3 0)). The 3_2 axis on the substructure origins must all disappear when the second origin is taken. This requires the different orientation of the CO_3 plane to be present in an ordered spiral chain. This is rejected because of a resulting O (3) – O (3) distance, 1.96 Å, as mentioned earlier. Taking the only possible origin, (004), and the ordering of CO_3 means the ordering of + and – cells, and there is only one independent way in their distribution; that is, three cells with one sign being different from the other two (++–, +–+, – –+, etc.) are all equivalent. The space group of the superstructure now is P32 rather than P3221.

To prove this model, intensities of 900 superstructure X-ray diffraction intensities were measured. No more than 10% of the weak peaks showed the observable symmetrical shape on a chart recorder. Based on all atomic parameters calculated from the substructure with isotropic temperature factors B = 1.0, the structure factors for observable superstructure reflections were calculated. The disagreement index R was 48%. It is very possible some of the atomic parameters may vary, though very little, in a superstructure. After the least-squares refinement using these inaccurate intensities the R decreased to 39%, but the interatomic distances of not only C-O but also Ca-O gave physically meaningless values. Another check may be to see if the space group is really $P3_2$ with no diad axis by examining the reflections (hkl) and its diad axis-related reflections. However, the inequality in the intensities was not clearly found because their accuracy is too low and, moreover, the difference of their structure factors is small even for the calculated ones. It is, therefore, not possible to prove this superstructure model experimentally

by X-ray diffraction. It is our belief that with neutron-diffraction intensity data, the ordered hydron positions maybe visualized and, thereby, the ordering of CO_3.

6. Preliminary Discussion of Vaterite-Calcium Carbonate Monohydrate Relationships

As mentioned in the introduction, evidence was found by McCauley and Roy[13] that there seemed to be an intimate relationship between the vaterite polymorph of $CaCO_3$ and $CaCO_3{\cdot}H_2O$. Further, it also seemed that in precipitation media with exceedingly high Ca concentration, $CaCO_3{\cdot}H_2O$ nucleates first but quickly becomes poisoned with the subsequent overgrowth of spherulitic vaterite. McCauley[12] also recognized a strong similarity between the X-ray powder patterns (Fig. 9) and lattice parameters of vaterite and $CaCO_3{\cdot}H_2O$. Moreover, vaterite spherulites can contain large amounts of water in intimate association.[14] Infrared spectra of $CaCO_3{\cdot}H_2O$ were also obtained and illustrated in Fig. 10.

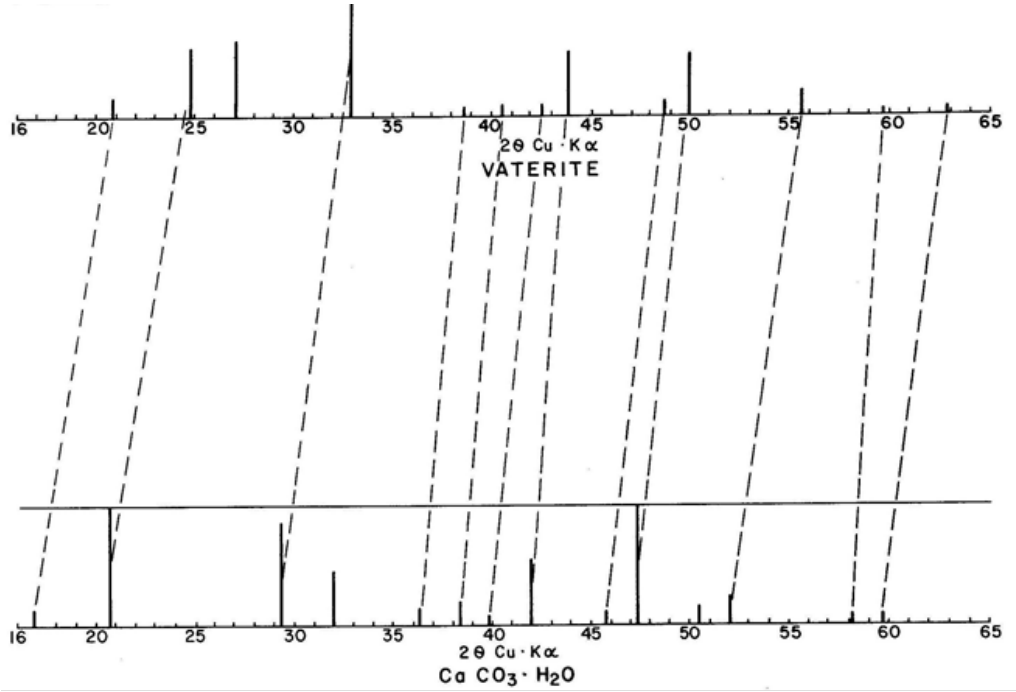

Fig. 9 X-ray powder diffraction patterns of vaterite and $CaCO_3{\cdot}H_2O$

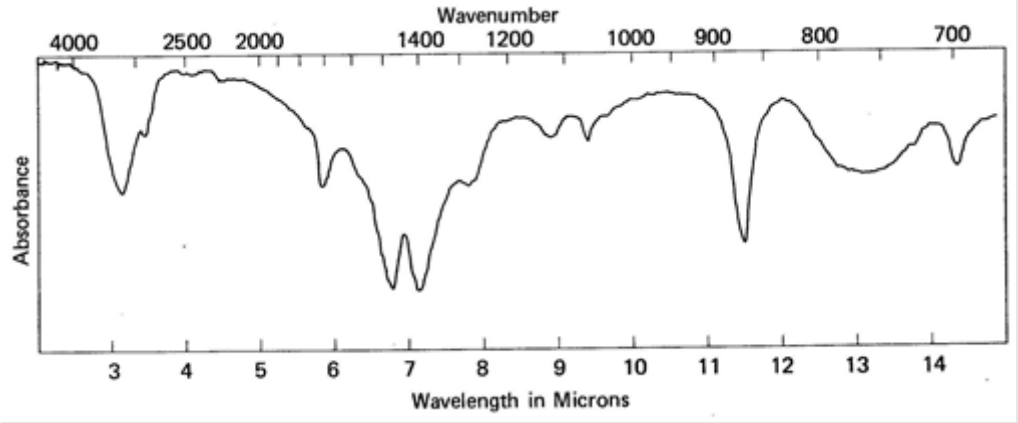

Fig. 10 Infrared spectra of $CaCO_3 \cdot H_2O$

Figure 11 illustrates the infrared spectra of the three $CaCO_3$ polymorphs. It appears there is a similarity to the vaterite polymorph, but not calcite or aragonite. Table 6 lists the infrared absorption spectra of $CaCO_3$ H_20.

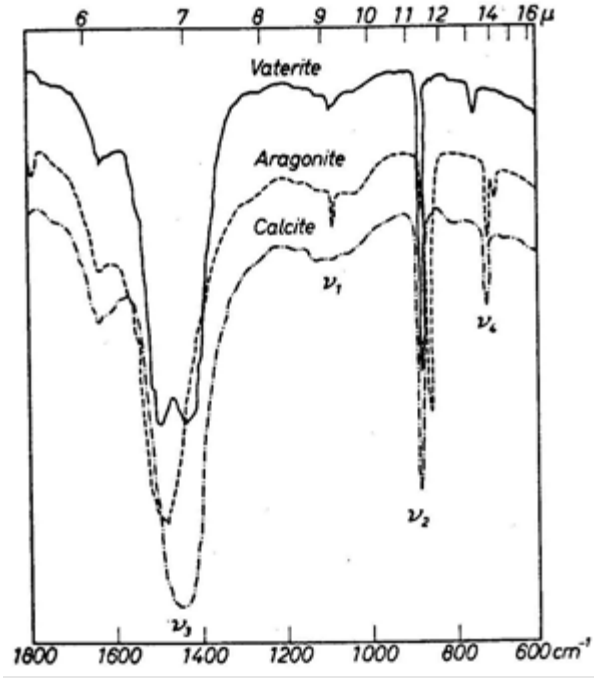

Fig. 11 Infrared spectra of the vaterite, calcite, and aragonite

Table 6 Infrared absorption spectra of $CaCO_3$ H_2O

Frequency (cm^{-1})	*x* (µm)	Intensity[a]	Identification
3195	3.13	m	H_2O
2907	3.44	mw, sh	H_2O
2439	4.10	vw, b	HCO_3
2232	4.48	vw	H_2O
1712	5.84	m	H_2O or a combination brand from CO_3
1477	6.77	s	…
1399	7.15	s	v_3 CO asymmetric stretching; indicates site symmetry C2v
1282	7.80	m, sh	…
1124	8.90	w, b	v_1 CO symmetric stretching
1064	9.40	w	…
870	11.50	ms, sp	v_2 CO_3 out-of-plane bending
768	13.03	wm, vb	H_2O hindered rotation and unesolvable v_4 or v_2
696	14.36	wm	V4 CO_3 in-plane bending

[a] m = medium, w = weak, s = strong, sh = shoulder, b = broad, vb = very broad

The following is a summary of the preliminary interpretation of the $CaCO_3 \cdot H_2O$ infrared spectra:

I. 1123 and 1064 cm^{-1} bands: Reflect asymmetry (low symmetry of molecule—indicates dipole moment) in the carbonate anion (v_1 splitting)

   1) Does not exist in calcite

   2) One band in aragonite

   3) Two bands (1005 and 1070 cm^{-1}) in vaterite

   4) Indicates H-band or different cation coordination about oxygen

II. 1477, 1399, and 1282 cm^{-1} bands: Reflect change in character of one or two C-O bonds (v_3 splitting)

   1) Aragonite and Calcite—*no*

   2) Vaterite—*yes*

   3) Pirssonite (Na_2Ca $(CO_3)_2 \cdot 2H_20$)—*yes*

   4) Two bands reflect differing C-O bands; one more at 7.8µ suggests H-

From the X-ray data and infrared spectroscopy, there appears to be close relationship between vaterite and $CaCO_3 \cdot H_2O$ and that it may be connected to the presence of hydrogen atoms in the structure in the form of water, HCO_3, or

hydroxyl (OH). However, at the end of the present work we could not come to a definitive conclusion.

Note: In some of the crystals, when viewed in transmitted light microscopy, there appeared to be very small faceted pores and/or unidentified inclusions. See Appendix B.

Approved for public release; distribution is unlimited.

7. References

1. Krauss F, Schriever W. Die hydrate calcium carbonate. Z Anorg Allg Chem. 1930;188:259–273. [German.]

2. Sapozhnikov DG, Tsvetkov AI. Precipitation of hydrous calcium carbonate on the bottom of Lake Issyk-Kul. Dokl Akad Nauk SSSR. 1959;124:131–133.

3. Carlstrom D. A crystallographic study of vertebrate otoliths. Bio Bull. 1963;125:441–462.

4. Marschner H. Hydrocalcite ($Ca\ CO_3 \cdot H_2O$) and mesguehonite ($Mg\ CO_3 \cdot 3H_2O$) in carbonate scales. Science. 1969;165:1119–1121.

5. Fischbeck R, Muller G. Monohydrocalcite, hydromagnesite, mesquehonite, dolomite, aragonite, and calcite in speleothems of the Fränkische Schweiz, Western Germany. Contrib Min Petr.1971;33(2):87–92.

6. Broughton PL. Monohydrocalcite in speleothems: an alternative interpretation. Contrib Min Petr. 1972;36(2):171–174.

7. Taylor GF. The occurrence of monohydrocalcite in two small lakes in the south-east of South Australia. Amer Miner. 1975;60(7–8):690–697.

8. Skinner, HCW, Osbaldiston GW, and Wilner AN. Monohydrocalcite in a guinea pig bladder stone, a novel occurrence. Amer Miner. 1977;62:273–277.

9. Halla F. Uber einige Versuche zur Dolomitsynthese durch doppelte Umlagerung Zentralbl. Mineral Geol Palaontal, Abt. A.1937;9:9–12. [German.]

10. Brooks R, Clark LM, Thurston EF. Calcium carbonate and its hydrates. Phil Trans Royal Soc. 1950;243A:145–167.

11. Baron G, Pesneau M. Sur l'existence et un mode de preparation du monohydrate de carbonate de calcium. C R. 1956;243:1217–1219. [French.]

12. McCauley JW. Control of nucleation, crystal growth, and doping of various calcium carbonate phases by the gel technique [master's thesis]. [University Park (PA)]: The Pennsylvania State University; 1965.

13. McCauley JW, Roy R. Controlled nucleation and crystal growth of various $CaCO_3$ phases by the silica gel technique. Amer Miner. 1974;59(9–10):947–963.

14. Donnay JDH, Donnay G. Optical determination of water content in spherulite vaterite. Acta Crystallographica. 1967;22:312–314.

15. McConnell JDC. Vaterite from ballycraigy, Lorne, Northern Ireland. Miner Mag. 1960;32:535–544.

16. Lippman F. Die Naturwissenshaften Heft. 1959. p. 553. [German.]

17. Sharma BD. Sodium bicarbonate and its hydrogen atom. Acta Crystallographica. 1965;1:818.

18. Meyer von HJ. Struktur und Fehlordnung des Vaterits. Zeitschrift Kristal. 1969;128:183–212. [German.]

Appendix A. Figure of Structure Factor Tables

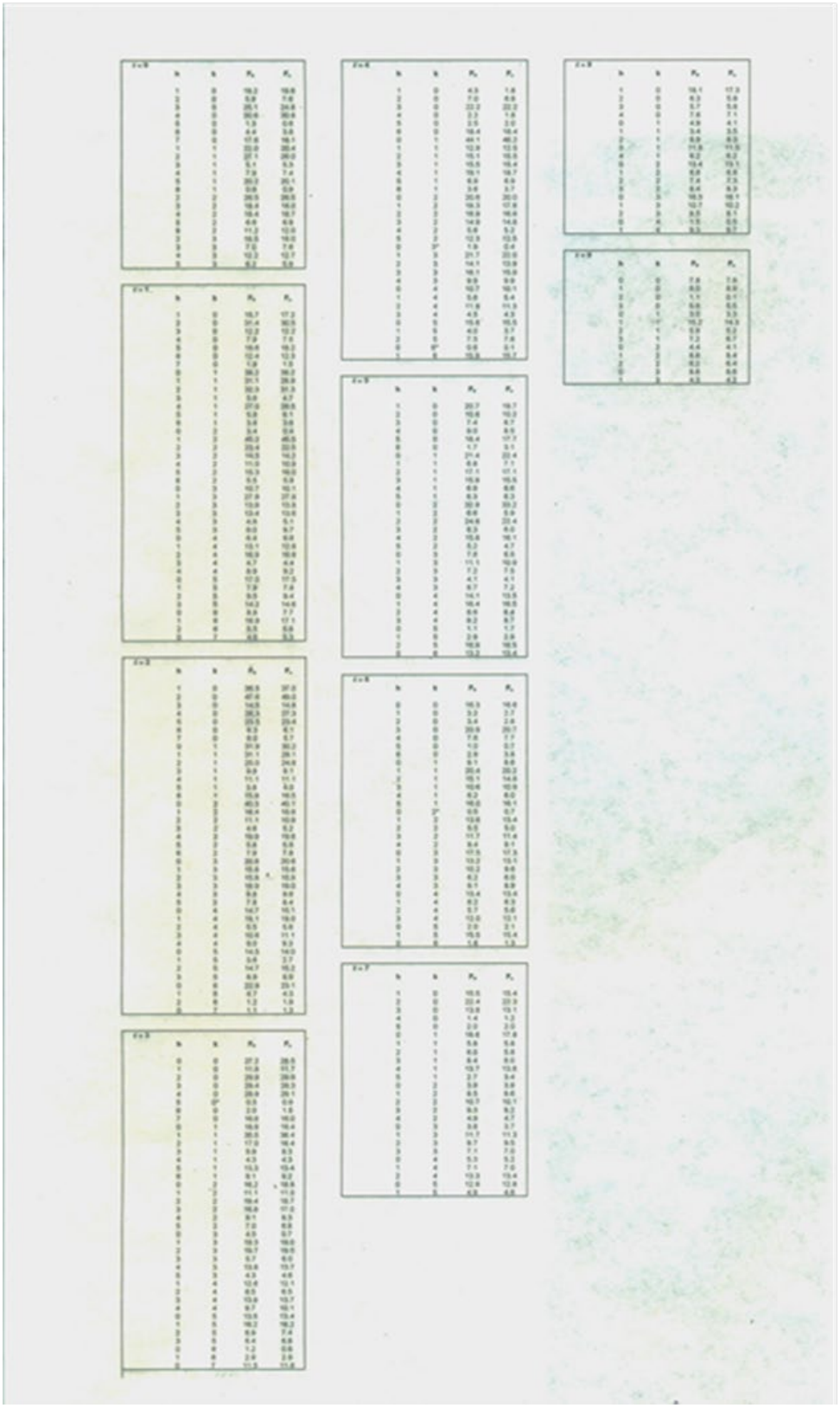

Fig. A-1 Image shows tables of observed and calculated structure factors based on final atomic parameters

Approved for public release; distribution is unlimited.

Appendix B. $CaCO_3 \cdot H_2O$ Optical Photomicrographs

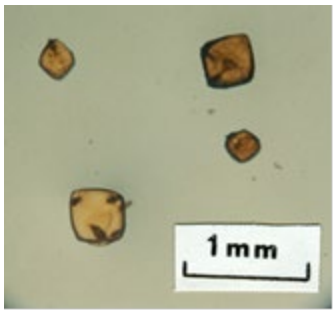

Fig. B-1 $CaCO_3 \cdot H_2O$ in transmitted plane light

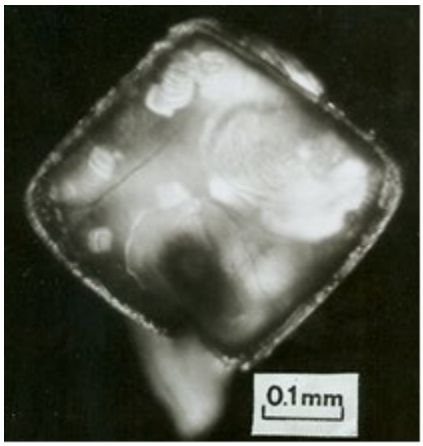

Fig. B-2 Halved crystal in crossed polarized light

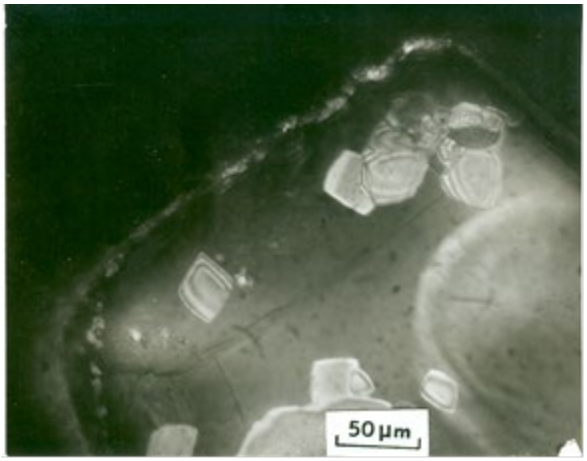

Fig. B-3 Magnified image of halved crystal with apparent inclusions

1 DEFENSE TECHNICAL
(PDF) INFORMATION CTR
DTIC OCA

2 DIR ARL
(PDF) IMAL HRA
RECORDS MGMT
RDRL DCL
TECH LIB

1 GOVT PRINTG OFC
(PDF) A MALHOTRA

2 Department Of Materials Science and Engineering
(1 PDF) Director Materials Research Institute
(1 HC) The Pennsylvania State University
ATTN: C. Randall
N-221 Millennium Science Complex
University Park, PA 16801

9 ARL
(4 PDF) RDRL WML B
R PESCE RODRIGUEZ
RDRL WM
J ZABINSKI
RDRL WMM
J BEATTY
(5 HC) JW MCCAULEY